

Oxidative DNA Cleavage, Formation of μ -1,1-Hydroperoxo Species, and Cytotoxicity of Dicopper(II) Complex Supported by a *p*-Cresol-Derived Amide-Tether Ligand

Yuki Kadoya,[†] Katsuki Fukui,[†] Machi Hata,[†] Risa Miyano,[†] Yutaka Hitomi,[†] Sachiko Yanagisawa,[‡] Minoru Kubo,[‡] and Masahito Kodera^{*,†}

[†]Department of Molecular Chemistry and Biochemistry, Doshisha University, Kyotanabe Kyoto 610-0321, Japan

[‡]Department of Life Science, University of Hyogo, Kouto 2-1, Ako Kamigori Hyogo 678-1297, Japan

Supporting Information

ABSTRACT: Metal complexes to promote oxidative DNA cleavage by H₂O₂ are desirable as anticancer drugs. A dicopper(II) complex of known *p*-cresol-derived methylene-tether ligand Hbcc [Cu₂(bcc)]³⁺ did not promote DNA cleavage by H₂O₂. Here, we synthesized a new *p*-cresol-derived amide-tether one, 2,6-bis(1,4,7,10-tetraazacyclododecyl-1-carboxamide)-*p*-cresol (Hbcamide). A dicopper(II) complex of the new ligand [Cu₂(μ -OH)(bcamide)]²⁺ was structurally characterized. This complex promoted the oxidative cleavage of supercoiled plasmid pUC19 DNA (Form I) with H₂O₂ at pH 6.0–8.2 to give Forms II and III. The reaction was largely accelerated in a high pH region. A μ -1,1-hydroperoxo species was formed as the active species and spectroscopically identified. The amide-tether complex is more effective in cytotoxicity against HeLa cells than the methylene-tether one.

Various metal complexes have been developed as anticancer drugs that block DNA replication through binding and/or cutting DNA.¹ In particular, platinum(II) complexes, for example, cisplatin² and its derivatives, such as oxaliplatin,³ lobaplatin,⁴ and nedaplatin,⁵ are capable of strongly binding DNA to block the replication and are clinically used as anticancer drugs.⁶ However, dosing of this type of anticancer drugs is accompanied by heavy side-effects and platinum-resistance problems.⁷ As one of the other types of anticancer drugs clinically used, bleomycin is known to cleave double-strand DNA (ds-DNA).⁸ It has a metal binding site as a pentadentate donor including an amide donor. The iron complex of bleomycin reacts with dioxygen molecules and/or hydrogen peroxide to form the activated bleomycin, proposed as a hydroperoxoiron(III) complex, to oxidatively cleave ds-DNA.⁹ This, however, causes the problem of side-effects in the lungs with the long-time use.¹⁰

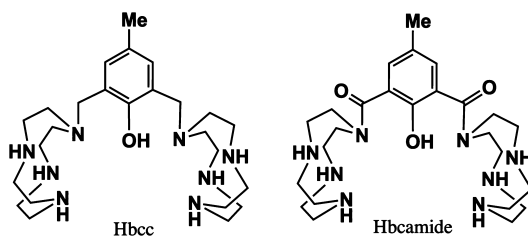
It is well-known that the microenvironment in the cancer cells is significantly different from that in normal cells.¹¹ As one of the key features of cancer cells, the concentration of reactive oxygen species (ROS) including H₂O₂ is relatively higher in cancer cells than in normal cells.¹² This is mainly caused by mitochondrial malfunction and increased metabolic activity of cancer cells.¹³ Thus, the overproduction of H₂O₂ in cancer

cells can be used to reduce the side-effect of anticancer drugs if we develop metal complexes capable of specifically activating H₂O₂ in cancer cells. So far, many complexes of copper,^{1a,14} iron,¹⁵ and various metals^{1d,16} have been reported to accelerate the oxidative DNA cleavage, but in most of them, large excess amounts of reducing reagents, such as 3-mercaptopropionic acid,^{14d} glutathione,^{14d,e} dithiothreitol,^{15b,d} and ascorbic acid,^{14a–c,15a} are essential. Amounts of reducing agents, however, are lower in cancer cells than in normal cells. Therefore, metal complexes capable of accelerating the oxidative DNA cleavage by H₂O₂ without reductants are desirable as anticancer drugs.

Previously, we reported that a dicopper(II) complex with *p*-cresol-derived methylene-tether ligand [Cu₂(bcc)](ClO₄)₃ (**1**) and related complexes accelerate hydrolytic DNA cleavage at pH 5–6,¹⁷ but **1** did not accelerate the DNA cleavage with H₂O₂. In this study, we synthesized a new *p*-cresol-derived amide-tether ligand 2,6-bis(1,4,7,10-tetraazacyclododecyl-1-carboxamide)-*p*-cresol (Hbcamide) and found that its dicopper(II) complex [Cu₂(μ -OH)(bcamide)](ClO₄)₂ (**2**) largely accelerates the oxidative DNA cleavage by H₂O₂ without reductants.

The methylene- and amide-tether ligands, Hbcc and Hbcamide, used in this study have two tetraazacyclododecane (cyclen) pendant groups tethered at 2,6-positions of *p*-cresol by –CH₂– and –CO– groups, respectively (Scheme 1). Hbcc and [Cu₂(bcc)](ClO₄)₂ (**1**) were prepared as previously reported.¹⁷ Hbcamide and [Cu₂(μ -OH)(bcamide)](ClO₄)₂ (**2**) are new compounds, and the synthetic details are shown

Scheme 1. Chemical Structures of Hbcc and Hbcamide



Received: July 13, 2019

in the Supporting Information. **Caution!** Perchlorate salts are potentially explosive and should be handled with great caution.

The amide-tether complex **2** was structurally characterized by X-ray analysis (see Table S1 for the crystallographic data and Table S2 for the selected bond distances and angles). The crystal structure of **1** was previously reported.¹⁷ ORTEP views of **1** and **2** are shown in Figure 1A and B, respectively. In **2**,

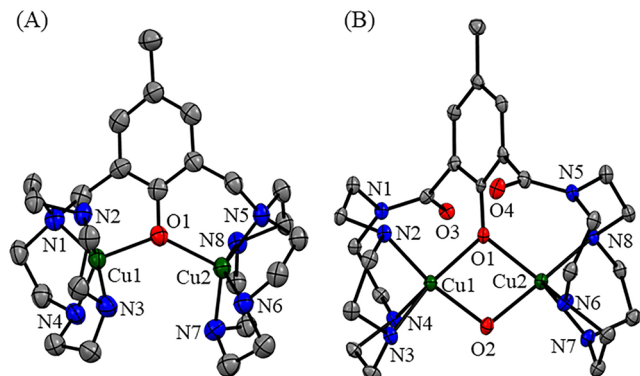


Figure 1. ORTEP diagrams of each cationic part of **1** (A) and **2** (B). Hydrogen atoms are omitted for clarity.

two Cu(II) ions are incorporated into a bcamide ligand and bridged by the endogenous μ -PhO and the exogenous μ -OH groups, where each Cu ion takes square pyramidal geometry with three N atoms of a pendant cyclen and two O atoms of the μ -OPh- μ -OH bridge. As previously reported, however, there is no μ -OH bridge in **1** where a Cu ion is coordinated by four N-atoms of pendant cyclen and the O-atom of the μ -PhO bridge. The Cu...Cu distance 3.047(11) Å of **2** is shorter than the 3.878(1) Å of **1**, due to the μ -PhO- μ -OH double bridge in **2**. The tether groups make these distinct differences in the Cu coordination structures between **1** and **2**.

The structure of **2** in an aqueous solution was examined by the spectroscopic studies. The ESI-MS spectrum of **2** in an aqueous solution is shown in Figure S1. The major peak appeared at m/z 745 corresponding to [bcamide + 2Cu(II) + OH + ClO₄]⁺. This shows that the μ -OPh- μ -OH bridge of **2** is kept in an aqueous solution. In the electronic absorption spectrum of **2** (Figure S2), two distinct bands appear at 326 and 390 nm assignable to HO⁻ and PhO⁻ to Cu(II) LMCT bands. These are similar to the LMCT bands at 340–400 nm reported for the related μ -OPh- μ -OH double bridged dicopper(II) complexes.^{17,18}

The reactivities of **1** and **2** in the DNA cleavage were examined using supercoiled plasmid pUC19 DNA (form I) as a substrate in the absence and presence of H₂O₂ under physiological pH 6.0–8.2 at 37 °C. Forms I, II, and III of DNA denote supercoiled close-circular, nicked circular, and linear double-strand DNA, respectively. Form I is converted to Forms II and III in the DNA cleavage. The amounts of Forms I, II, and III were analyzed by agarose gel electrophoresis. The gel patterns and time courses are shown in Figures S3–S12 and Tables S3–S7. The decreases of percent of Form I versus time in the reactions using **1** and **2** at pH 6.0 in the presence of H₂O₂ (0.5 mM) are shown in Figure 2. The decreased rate of Form I in the reaction of the methylene-tether complex **1** in the presence of H₂O₂ is exactly the same as that in the absence of H₂O₂. Thus, **1** did not accelerate the oxidative DNA cleavage with H₂O₂ at all. The decrease of percent of Form I in

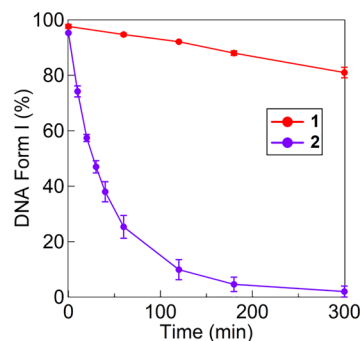


Figure 2. Time courses for the decrease of percent of Form I upon reaction of pUC19 DNA (50 μ M bp) with **1** (red) or **2** (purple; 50 μ M) in the presence of H₂O₂ (0.5 mM) at pH 6.0 (10 mM MES, 10 mM NaCl) at 37 °C.

the reaction of **1** is caused by hydrolytic DNA cleavage as previously reported.¹⁷ On the other hand, in the presence of H₂O₂, the amide-tether complex **2** significantly accelerated the decrease of percent of Form I as shown in Figure 2. The hydrolytic DNA cleavage activity of **2** was almost the same as that of **1** (see Figure S8). The oxidative DNA cleavage is confirmed by the fact that Form III produced in the reaction is not converted to form II by treatment with T4 DNA ligase (Figure S20). Thus, **2** specifically promoted oxidative DNA cleavage with H₂O₂, where **2** activates H₂O₂ for the oxidative DNA cleavage because H₂O₂ did not cleave DNA by itself in the absence of **2**. Moreover, the oxidative DNA cleavage rate increased with an increase of concentrations of both **2** and H₂O₂ as shown in Figures S9 and S10 and Tables S6. These results suggest that the reaction proceeds via formation of the active species from **2** and H₂O₂. The active species was spectroscopically identified as described below.

The pH dependence of the oxidative DNA cleavage was further examined by using the amide-tether complex **2** in detail. A decrease of percent of Form I and increase of percent of Form III in the reactions at pH 6.0, 7.4, and 8.2 in the presence of H₂O₂ (0.3 mM) are shown in Figure S4. As shown in Figure S4A, the decrease of percent of Form I is accelerated at higher pH. Moreover, it was found that the formation rate of Form III is drastically enhanced at higher pH as shown in Figure S4B. At pH 8.2, 50% of form I was converted to Form III in 5 h, but an almost negligible amount of Form III was detected at pH 6.0. This suggested that the formation of the active species is accelerated at high pH. Form III is a linear DNA formed by the cleavage of two phosphate-ester main chains at the near positions of ds-DNA. Actually, **2** showed relatively high oxidative DNA cleavage activity in the presence of H₂O₂ as compared with a tricopper complex reported before.¹⁴ Thus, the active species has a strong oxidation ability capable of cleaving ds-DNA, and this is similar to the activated bleomycin.

The oxidative DNA cleavage studies in the presence of various inhibitors, NaN₃ (singlet oxygen scavenger), DMSO (hydroxy radical scavenger), and KI (superoxide scavenger), were also carried out to identify the active species that may be formed in the reaction of **2** with H₂O₂. The results are shown in Figures S11 and S12 and Tables S7. The addition of NaN₃ (0.5 mM) and DMSO (0.5 mM) to the reaction of **2** slightly enhanced the DNA cleavage but did not inhibit at all, suggesting that both a singlet oxygen and a diffusible hydroxy radical are not the active species in the DNA cleavage. The

reaction was only slightly inhibited when KI (0.5 mM) was added to the reaction of **2**. In this case, KI acts as a reductant, and thus, H_2O_2 by itself and a Cu-bonded peroxide complex are possible candidates as the active species in the DNA cleavage. The former is not the active species because the DNA cleavage did not occur when only H_2O_2 was used. Both **2** and H_2O_2 are essential for DNA cleavage.

To detect the active species, the reactions of complexes, **1** and **2**, with H_2O_2 were monitored on the electronic absorption spectra. Upon the addition of H_2O_2 to a solution of the methylene-tether complex **1**, any spectral change did not occur (Figure S13), showing that **1** does not bind H_2O_2 . This is consistent with no reactivity of **1** in the oxidative DNA cleavage with H_2O_2 . On the other hand, the amide-tether complex **2** reacted with H_2O_2 to give clear bands at 340 ($\epsilon = 5600 \text{ M}^{-1} \text{ cm}^{-1}$) and 398 ($\epsilon = 4800 \text{ M}^{-1} \text{ cm}^{-1}$) nm (Figure S13). The band at 398 nm is similar to HO_2^- to Cu(II) LMCT bands around 390–400 nm reported for various μ -1,1-hydroperoxodicopper(II) complexes,¹⁹ indicating that a μ -1,1-hydroperoxodicopper(II) species $[\text{Cu}_2(\text{O}_2\text{H})(\text{bcamide})]^{2+}$ (**3**) may be formed in the reaction of **2** with H_2O_2 . Formation of **3** was not affected by Et_3N , small phosphate anions, and N_3^- ion as shown in Figure S14B–E. The formation of **3** is shown by CSI MS spectra, having two major peaks at m/z 331 and 761 corresponding to $[\text{bcamide} + 2\text{Cu}(\text{II}) + \text{O}_2\text{H}]^{2+}$ and $[\text{bcamide} + 2\text{Cu}(\text{II}) + \text{O}_2\text{H} + \text{ClO}_4]^{+}$, respectively (Figure S15). When ^{18}O -labeled $\text{H}_2^{18}\text{O}_2$ was used instead of $\text{H}_2^{16}\text{O}_2$, these shifted to m/z 333 and 765, demonstrating that two O atoms of **3** come from H_2O_2 (Figure S16). The CSI MS spectrum measured upon the reaction of **2** with H_2O_2 in H_2O gave two major peaks at m/z 331 and 761 (Figure S21), showing that **3** is formed in the oxidative DNA cleavage in H_2O . Moreover, the formation of **3** in H_2O was also observed on the electronic absorption spectrum (Figure S22).

The resonance Raman spectra of **3** are shown in Figure 3. A clear band appeared at 897 cm^{-1} upon reaction of **2** with

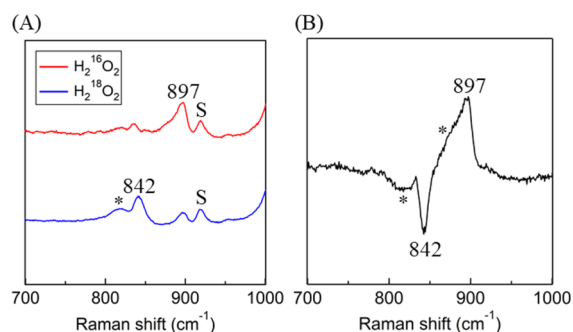


Figure 3. (A) Resonance Raman spectra of **3** prepared from **2** and excess amounts of $\text{H}_2^{16}\text{O}_2$ (red) or $\text{H}_2^{18}\text{O}_2$ (blue) in MeOH at -30°C with excitation at 405 nm. (B) A difference spectrum of A. S and * mean solvent and H_2O_2 .

$\text{H}_2^{16}\text{O}_2$. By using $\text{H}_2^{18}\text{O}_2$ instead of $\text{H}_2^{16}\text{O}_2$, this band shifted to 842 cm^{-1} due to the isotope shift (55 cm^{-1}). These data are similar to the $\nu_{\text{O}-\text{O}}$ band at 892 cm^{-1} and an isotope shift of 52 cm^{-1} of μ -1,1-hydroperoxodicopper(II) complex with the *p*-cresol derived ligand.²⁰ Thus, **3** is proposed as a μ -1,1-hydroperoxodicopper(II) complex shown in Figure 4.

The reaction of **3** (0.25 mM) with guaiacol (7.5 mM) was monitored by the electronic absorption spectral change (Figure S17), where **3** readily oxidized guaiacol to give corresponding

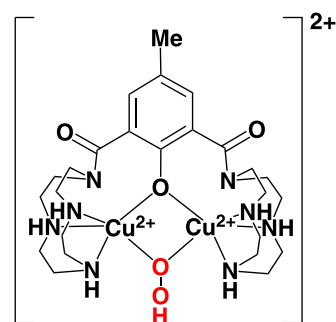


Figure 4. A proposed chemical structure of the μ -1,1-hydroperoxodicopper(II) complex **3**.

tetraquaiacol as an oxidized product, and the typical absorption bands appeared at 412 and 470 nm.²¹ The concentration of tetraquaiacol obtained was estimated as 0.05 mM from absorbance at 470 nm ($\epsilon = 26.6 \text{ mM}^{-1} \text{ cm}^{-1}$;^{21a,22} Figure S17B) where 0.2 mM of **3** was used to form tetraquaiacol because 4 equiv of **3** is consumed to convert guaiacol to tetraquaiacol. Thus, the yield of the tetraquaiacol was ca. 80% on the basis of **3** used. These results clearly show **3** is the active species in the reaction. The increase of tetraquaiacol was monitored at 500 nm, and the reaction rate was estimated as $2.93 \times 10^{-2} \text{ min}^{-1}$ (Figure S17C). Guaiacol was not oxidized only by H_2O_2 . These results indicate that **3** is the direct oxidant in the oxidative DNA cleavage.

Finally, we examined cytotoxicity of the methylene-tether complex **1** and the amide tether complex **2** against HeLa cells. HeLa is a human cell line derived from cervical cancer cells taken from Henrietta Lacks, a patient who died of cancer. The cytotoxicity was determined by means of MTT assay.²³ The details are described in the Supporting Information. The IC_{50} values (Table S8 and Figure S20) clearly show that **2** is more effective in the cytotoxicity than **1**. This is proportional to the high DNA cleavage ability of **2**.

In this study, we synthesized a new amide-tether ligand and its dicopper(II) complex $[\text{Cu}_2(\mu\text{-OH})(\text{bcamide})](\text{ClO}_4)_2$ (**2**) and found that the amide-tether complex **2** largely accelerated the oxidative DNA cleavage with H_2O_2 . Moreover, **2** reacts with H_2O_2 to form the active species, which was spectroscopically identified as a μ -1,1-hydroperoxodicopper(II) complex **3**. These results may shed light on the development of new anticancer drugs to reduce the heavy side-effect.

■ ASSOCIATED CONTENT

Supporting Information

The Supporting Information is available free of charge on the ACS Publications website at DOI: 10.1021/acs.inorgchem.9b02093.

Detailed experimental procedures, syntheses of ligands and complexes, Figures S1–S22, Tables S1–S8, and Schemes S1 and S2 (PDF)

Accession Codes

CCDC 1937747 contains the supplementary crystallographic data for this paper. These data can be obtained free of charge via www.ccdc.cam.ac.uk/data_request/cif, or by emailing data_request@ccdc.cam.ac.uk, or by contacting The Cambridge Crystallographic Data Centre, 12 Union Road, Cambridge CB2 1EZ, UK; fax: +44 1223 336033.

AUTHOR INFORMATION

Corresponding Author

*E-mail: mkodera@mail.doshisha.ac.jp.

ORCID

Yutaka Hitomi: 0000-0002-2448-296X

Masahito Kodera: 0000-0001-9979-1743

Notes

The authors declare no competing financial interest.

ACKNOWLEDGMENTS

This work was supported by MEXT-Supported Program of the Strategic Research Foundation at Private University, 2015–2019.

REFERENCES

- (1) (a) Santini, C.; Pellei, M.; Gandin, V.; Porchia, M.; Tisato, F.; Marzano, C. Advances in Copper Complexes as Anticancer Agents. *Chem. Rev.* **2014**, *114*, 815–862. (b) Kettenmann, S. D.; Louka, F. R.; Marine, E.; Fischer, R. C.; Mautner, F. A.; Kulak, N.; Massoud, S. S. Efficient Artificial Nucleases for Mediating DNA Cleavage Based on Tuning the Steric Effect in the Pyridyl Derivatives of Tripod Tetraamine-Cobalt(II) Complexes. *Eur. J. Inorg. Chem.* **2018**, *2018*, 2322–2338. (c) Dasari, S.; Bernard Tchounwou, P. Cisplatin in cancer therapy: Molecular mechanism of action. *Eur. J. Pharmacol.* **2014**, *740*, 364–378. (d) Copeland, K. D.; Fitzsimons, M. P.; Houser, R. P.; Barton, J. K. DNA Hydrolysis and Oxidative Cleavage by Metal-Binding Peptides Tethered to Rhodium Intercalators. *Biochemistry* **2002**, *41*, 343–356.
- (2) (a) Johnstone, T. C.; Suntharalingam, K.; Lippard, S. J. The Next Generation of Platinum Drugs: Targeted Pt(II) Agents, Nanoparticle Delivery, and Pt(IV) Prodrugs. *Chem. Rev.* **2016**, *116*, 3436–3486. (b) Rosenberg, B. Fundamental Studies With Cisplatin. *Cancer* **1985**, *55*, 2303–2316.
- (3) Kidani, Y.; Inagaki, K.; Iigo, M.; Hoshi, A.; Kuretani, K. Antitumor activity of 1,2-diaminocyclohexaneplatinum complexes against Sarcoma-180 ascites form. *J. Med. Chem.* **1978**, *21*, 1315–1318.
- (4) McKeage, M. J. Lobaplatin: a new antitumor platinum drug. *Expert Opin. Invest. Drugs* **2001**, *10*, 119–128.
- (5) Shimada, M.; Itamochi, H.; Kigawa, J. Nedaplatin: a cisplatin derivative in cancer chemotherapy. *Cancer Manage. Res.* **2013**, *5*, 67–76.
- (6) Jamieson, E. R.; Lippard, S. J. Structure, Recognition, and Processing of Cisplatin-DNA Adducts. *Chem. Rev.* **1999**, *99*, 2467–2498.
- (7) Florea, A.-M.; Büsselberg, D. Cisplatin as an Anti-Tumor Drug: Cellular Mechanisms of Activity, Drug Resistance and Induces Side Effects. *Cancers* **2011**, *3*, 1351–1371.
- (8) (a) Burger, R. M. Cleavage of Nucleic Acids by Bleomycin. *Chem. Rev.* **1998**, *98*, 1153–1169. (b) Abraham, A. T.; Zhou, X.; Hecht, S. M. DNA Cleavage by Fe(II)•Bleomycin Conjugated to a Solid Support. *J. Am. Chem. Soc.* **1999**, *121*, 1982–1983. (c) Huang, S.-X.; Feng, Z.; Wang, L.; Galm, U.; Wendt-Pienkowski, E.; Yang, D.; Tao, M.; Coughlin, J. M.; Duan, Y.; Shen, B. A Designer Bleomycin with Significantly Improved DNA Cleavage Activity. *J. Am. Chem. Soc.* **2012**, *134*, 13501–13509.
- (9) (a) Decker, A.; Chow, M. S.; Kemsley, J. N.; Lehnert, N.; Solomon, E. I. Direct Hydrogen-Atom Abstraction by Activated Bleomycin: An Experimental and Computational Study. *J. Am. Chem. Soc.* **2006**, *128*, 4719–4733. (b) Liu, L. V.; Bell, C. B., III; Wong, S. D.; Wilson, S. A.; Kwak, Y.; Chow, M. S.; Zhao, J.; Hodgson, K. O.; Hedman, B.; Solomon, E. I. Definition of the intermediates and mechanism of the anticancer drug bleomycin using nuclear resonance vibrational spectroscopy and related methods. *Proc. Natl. Acad. Sci. U. S. A.* **2010**, *107*, 22419–22424.
- (10) Adamson, I. Y. R. Pulmonary toxicity of bleomycin. *Environ. Health Perspect.* **1976**, *16*, 119–126.
- (11) Zhou, D.; Shao, L.; Spitz, D. R. Reactive Oxygen Species in Normal and Tumor Stem Cells. *Adv. Cancer Res.* **2014**, *122*, 1–67.
- (12) (a) Nogueira, V.; Hay, N. Molecular Pathways: Reactive Oxygen Species Homeostasis in Cancer Cells and Implications for Cancer Therapy. *Clin. Cancer Res.* **2013**, *19*, 4309–4314. (b) Szatrowski, T. P.; Nathan, C. F. Production of Large Amounts of hydrogen peroxide by Human Tumor Cells. *Cancer Res.* **1991**, *51*, 794–798.
- (13) (a) Aykin-Burns, N.; Ahmad, I. M.; Zhu, Y.; Oberley, L. W.; Spitz, D. R. Increased levels of superoxide and H₂O₂ mediate the differential susceptibility of cancer cells versus normal cells to glucose deprivation. *Biochem. J.* **2009**, *418*, 29–37. (b) Ishii, N.; Fujii, M.; Hartman, P. S.; Tsuda, M.; Yasuda, K.; Senoo-Matsuda, N.; Yanase, S.; Ayusawa, D.; Suzuki, K. A mutation in succinate dehydrogenase cytochrome *b* causes oxidative stress and ageing in nematodes. *Nature* **1998**, *394*, 694–697.
- (14) (a) Tu, C.; Shao, Y.; Gan, N.; Xu, Q.; Guo, Z. Oxidative DNA Strand Scission Induced by a Trinuclear Copper(II) Complex. *Inorg. Chem.* **2004**, *43*, 4761–4766. (b) González-Alvarez, M.; Alzuet, G.; Borrás, J.; Macías, B.; Castiñeiras, A. Oxidative Cleavage of DNA by a New Ferromagnetic Linear Trinuclear Copper(II) Complex in the Presence of H₂O₂/Sodium Ascorbate. *Inorg. Chem.* **2003**, *42*, 2992–2998. (c) Santra, B. K.; Reddy, P. A. N.; Neelakanta, G.; Mahadevan, S.; Nethaji, M.; Chakravarty, A. R. Oxidative cleavage of DNA by a dipyridoquinoxaline copper(II) complex in the presence of ascorbic acid. *J. Inorg. Biochem.* **2002**, *89*, 191–196. (d) Borrás, J.; Alzuet, G.; Gonzalez-Alvarez, M.; Garcia-Gimenez, J. L.; Macias, B.; Liu-Gonzalez, M. Efficient DNA Cleavage Induced by Copper(II) Complexes of Hydrolysis Derivatives of 2,4,6-Tris(2-pyridyl)-1,3,5-triazine in the Presence of Reducing Agents. *Eur. J. Inorg. Chem.* **2007**, *2007*, 822–834. (e) Vaidyanathan, V. G.; Nair, B. U. Oxidative cleavage of DNA by tridentate copper (II) complex. *J. Inorg. Biochem.* **2003**, *93*, 271–276.
- (15) (a) El Amrani, F. B. A.; Perello, L.; Real, J. A.; Gonzalez-Alvarez, M.; Alzuet, G.; Borrás, J.; Garcia-Granda, S.; Montejo-Bernardo, J. Oxidative DNA cleavage induced by an iron(III) flavonoid complex: Synthesis, crystal structure and characterization of chlorobis(flavonolate)(methanol) iron(III) complex. *J. Inorg. Biochem.* **2006**, *100*, 1208–1218. (b) Li, Q.; van den Berg, T. A.; Feringa, B. L.; Roelfes, G. Mononuclear Fe(II)-N4Py complexes in oxidative DNA cleavage: structure, activity and mechanism. *Dalton Trans* **2010**, *39*, 8012–8021. (c) Roelfes, G.; Branum, M. E.; Wang, L.; Que, L., Jr.; Feringa, B. L. Efficient DNA Cleavage with an Iron Complex without Added Reductant. *J. Am. Chem. Soc.* **2000**, *122*, 11517–11518. (d) van den Berg, T. A.; Feringa, B. L.; Roelfes, G. Double strand DNA cleavage with a binuclear iron complex. *Chem. Commun.* **2007**, *2*, 180–182.
- (16) (a) Satharaj, G.; Kiruthika, M.; Weyhermuller, T.; Unni Nair, B. Oxidative Cleavage of DNA Ruthenium(II) Complexes Containing a Ferrocene/Non-Ferrocene Conjugated Imidazole Phenol Ligand. *Organometallics* **2012**, *31*, 6980–6987. (b) Mack, D. P.; Dervan, P. B. Nickel-mediated sequence-specific oxidative cleavage of DNA by a designed metalloprotein. *J. Am. Chem. Soc.* **1990**, *112*, 4604–4606.
- (17) Kodera, M.; Kadoya, Y.; Aso, K.; Fukui, K.; Nomura, A.; Hitomi, Y.; Kitagishi, H. Acceleration of Hydrolytic DNA Cleavage by Dicopper(II) Complexes with *p*-Cresol-Derived Dinucleating Ligands at Slightly Acidic pH and Mechanistic Insights. *Bull. Chem. Soc. Jpn.* **2019**, *92*, 739–747.
- (18) (a) Rey, N. A.; Neves, A.; Bortoluzzi, A. J.; Pich, C. T.; Terenzi, H. Catalytic Promiscuity in Biomimetic Systems: Catecholase-like Activity, Phosphatase-like Activity, and Hydrolytic DNA Cleavage Promoted by a New Dicopper(II) Hydroxo-Bridged Complex. *Inorg. Chem.* **2007**, *46*, 348–350. (b) Amudha, P.; Kandaswamy, M.; Govindasamy, L.; Velmurugan, D. Synthesis and Characterization of New Symmetrical Binucleating Ligands and Their μ -Phenoxo-Bridged Bicopper(II) Complexes: Structural, Electrochemical, and Magnetic Studies. *Inorg. Chem.* **1998**, *37*, 4486–4492.

(19) (a) Root, D. E.; Mahroof-Tahir, M.; Karlin, K. D.; Solomon, E. I. Effect of Protonation on Peroxo-Copper Bonding: Spectroscopic and Electronic Structure Study of $[\text{Cu}_2(\text{UN-O})(\text{OOH})]^{2+}$. *Inorg. Chem.* **1998**, *37*, 4838–4848. (b) Kindermann, N.; Dechert, S.; Demeshko, S.; Meyer, F. Proton-Induced, Reversible Interconversion of a μ -1,2-Peroxo and a μ -1,1-Hydroperoxo Dicopper(II) Complex. *J. Am. Chem. Soc.* **2015**, *137*, 8002–8005. (c) Battaini, G.; Monzani, E.; Perotti, A.; Para, C.; Casella, L.; Santagostini, L.; Gullotti, M.; Dillinger, R.; Näther, C.; Tuczek, F. A Double Arene Hydroxylation Mediated by Dicopper-Hydroperoxide Species. *J. Am. Chem. Soc.* **2003**, *125*, 4185–4198.

(20) (a) Li, L.; Narducci Sarjeant, A. A.; Vance, M. A.; Zakharov, L. N.; Rheingold, A. L.; Solomon, E. I.; Karlin, K. D. Exogenous Nitrile Substrate Hydroxylation by a New Dicopper-Hydroperoxide Complex. *J. Am. Chem. Soc.* **2005**, *127*, 15360–15361.

(21) (a) Hong, J.; Wang, W.; Huang, K.; Yang, W.-Y.; Zhao, Y.-X.; Xiao, B.-L.; Gao, Y.-F.; Moosavi-Movahedi, Z.; Ahmadian, S.; Bohlooli, M.; Saboury, A. A.; Ghourchian, H.; Sheibani, N.; Moosavi-Movahedi, A. A. A self-assembled nano-cluster complex based on cytochrome *c* and nafion: An efficient nanostructured peroxidase. *Biochem. Eng. J.* **2012**, *65*, 16–22. (b) Hwang, S.; Lee, C.-H.; Ahn, I.-S. Product identification of guaiacol oxidation catalyzed by manganese peroxidase. *J. Ind. Eng. Chem.* **2008**, *14*, 487–492.

(22) Lopes, L. C.; Brandao, I. V.; Sanchez, O. C.; Franceschi, E.; Borges, G.; Dariva, C.; Fricks, A. T. Horseradish peroxidase biocatalytic reaction monitoring using Near-Infrared (NIR) Spectroscopy. *Process Biochem.* **2018**, *71*, 127–133.

(23) Mosmann, T. Rapid colorimetric assay for cellular growth and survival: Application to proliferation and cytotoxicity assays. *J. Immunol. Methods* **1983**, *65*, 55–63.